Electronic Supplementary Material (ESI) for Journal of Materials Chemistry A.

Supporting Electronic Information

Electrochemical Synthesis of Ammonia from Nitric Oxide in a Membrane Electrode Assembly Electrolyzer Over Dual Fe-Ni Single Atom Catalyst

*Sridhar Sethuram Markandaraj, Dinesh Dhanabal and Sangaraju Shanmugam**

Department of Energy Science & Engineering,

Daegu Gyeongbuk Institute of Science & Technology (DGIST),

Daegu 42988, Republic of Korea

Tel.: +82 53 785 6413; fax: +82 53 785 6402.

E-mail: sangarajus@dgist.ac.kr

Experimental Section

Electrochemical characterization:

The eNORR study was conducted using a potentiostat (Biologic, VSP) with batch electrolyzer and MEA electrolyzer. For the ENOR of batch electrolyzer, an air-tight H-type cell separated by the Nafion-212 membrane was used. The catalyst loaded GDE, graphite rod, and Ag/AgCl were used as working, counter and reference electrodes, respectively. All the potential values were converted to RHE scale using the Nernst relation ($E_{RHE} = E_{WE} + E^{\circ}_{Ag/AgCl} + 0.059$ pH, $E^{\circ}_{Ag/AgCl} = 0.197$ V). To conduct electrolysis, the two chambers of the H-cell were filled with HCl (0.1 M). The high purity Ar gas was purged at the cathodic compartment for at least 1 h to remove the dissolved oxygen. The nitric oxide (NO) was used as a source gas and purged with a suitable sparger in the cathode compartment for the eNORR analysis. To capture the possible NH_3 gas product, the tail gas of the catholyte chamber was trapped in an acidic HCl solution. After the electrolysis, the excess dissolved NO molecules were removed by purging the Ar gas.

The MEA electrolyzer with an active area of 5 cm^2 was used. The catalyst-coated GDE as cathode layer, RuO_2 as anode layer and NRE-212 as membrane were employed. We operated the cell under ambient temperature and pressure. Humidified NO gas was supplied from the back side of the cathode layer, and HCl (0.1 M) as anolyte circulated in the anode side. The humidity of the NO gas is controlled by adjusting the saturation humidifier temperatures of 40°C, 50°C, 55°C, and 60°C which corresponds to the relative humidification (RH) values of 37%, 62%, 79%, and 100%, respectively. The gas outlet from the catholyte is connected to the acid reservoir to dissolve the formed NH_3 gas and used for product quantification. The electrochemical impedance spectroscopy (EIS) was analyzed by applying an amplitude voltage of 10 mV over a frequency range of 1 Hz to 100 kHz.

Nafion membrane pretreatment:

The Nafion-212 membrane was pretreated with H_2O_2/ DIW mixture (1:5) at 90 °C for 1 h to remove the organic impurities.[2] It is followed by rinsing and boiling in DIW at 100 °C for 1 h. Then, the membrane was boiled at 135 °C in H_2SO_4 (1 M) for 1 h for protonation. Finally, the membrane was transferred to boiling DIW for 1 h, followed by storing the membrane in DIW container.

Electrode fabrication for half-cell test:

The spray coating technique was applied to load the catalyst on GDE (1 x 1 cm^2). The catalyst loading of 2 mg cm^{-2} loading was maintained. The catalyst ink was prepared by dispersing 10 mg of catalyst in IPA (800 µL), DIW (200 µL), and Nafion solution (5 wt%, 100 µL). The resultant solution is sonicated for 1 h to form a homogeneous ink.

Ink, catalyst layer and MEA fabrication for full-cell test:

The brush coating technique was employed to prepare the catalyst layer on the GDE electrodes. The cathode catalyst ink was prepared by dispersing 5 mg of catalyst (FeNi-NCNT) in IPA (400 µL), DIW (100 µL), and Nafion solution (5 wt%, 50 µL). The anode catalyst ink was prepared by dispersing 5 mg of catalyst (RuO_2) in IPA (400 µL), DIW (100 µL), and Nafion solution (5 wt%, 25 µL). Then, the resultant catalyst dispersion was sonicated for 1 h to form a homogeneous ink. The active geometrical area was 5 cm^2 with catalyst loading of 1 mg cm^{-2}. Next, the membrane electrode assembly (MEA) was fabricated by hot pressing both electrodes and pretreated membrane at 130 °C for 2 min by applying 2 MPa.

Products quantification:

The possible products produced during eNORR are NH_3, N_2H_4, NH_2OH, N_2O, N_2 and H_2. During the entire electrolysis, the gaseous products such as N_2O, N_2 and H_2 were not considered. However, to examine possible NH_3 gas formation, the tail gas from the reactor was connected with the acid trap. NH_3 was quantified using the indophenol blue method and ^{1}H-NMR. NH_2OH and N_2H_4 were estimated using the corresponding colorimetry methods.

Quantification of NH_3: The indophenol blue method was used to calculate the NH_3 concentration.[3] After the electrolysis period, 2 mL of analyte was mixed with Solution A (2 mL), Solution B (1 mL), and Solution C (200 μL) (Solution A: NaOH (1 M) containing salicylic acid (5 wt.%), trisodium citrate dihydrate (5 wt.%); solution B: sodium hypochlorite (0.05 M); Solution C: 1 wt.% Sodium nitroprusside). The absorption at 655 nm was taken using UV-vis spectrophotometer after 1 h of incubation in the dark. Similarly, NH_4Cl of known concentration was dissolved in HCl (0.1 M) to obtain a standard calibration plot. To quantify ammonia using ^{1}H-NMR, analyte (400 μL) was blended with H_2SO_4 (50 μL, 4 M) and DMSO-d_6 (50 μL). Maleic acid of known concentration was added as an internal standard to obtain quantifiable data. At the same time, the NH_3 was calculated by integrating the triplet with respect to the standard maleic acid peak (6.25 δ). In the same way, ^{1}H-NMR spectra of electrolyte-containing known concentrations of NH_4Cl were used to draw a standard plot.

Quantification of N_2H_4: The Watt and Chrisp method is used to quantify the concentration of N_2H_4 in the electrolyte.[4] Initially, a color reagent is a solution of para-(dimethylamino) benzaldehyde (5.99 g) in concentrated HCl (30 mL) and ethanol (300 mL). Analyte (2 mL) was diluted with DIW and blended with KOH (1 mL, 1 M), followed by adding color reagent (5 mL).

The resultant sample is incubated in the dark for about 10 min, then the absorbance at a wavelength of 455 nm was taken to calculate the amount of N_2H_4. In the same way, the absorption-concentration curve was acquired by taking a known amount of N_2H_4 in HCl (0.1 M) electrolyte.

Quantification of NH_2OH: NH_2OH was quantified by a colorimetric method.[5] In brief, analyte (1 mL), phosphate buffer solution (1 mL, 0.05 M), DIW (0.8 mL), trichloroacetic acid (0.2 mL), 8-quinolinol (1 mL) were mixed and swirled slightly, followed by adding Na_2CO_3 (1 mL, 1 M). The resultant solution was shaken vigorously with a stopper; finally, the vial was maintained in a boiling water bath for color development. Then, the absorbance at 705 nm was taken to evaluate the concentration of NH_2OH, after the blend was cooled at room temperature for 15 min. Following the same method, a calibration curve was derived by evaluating a series of NH_2OH solutions in the concentration range of 6-40 μM.

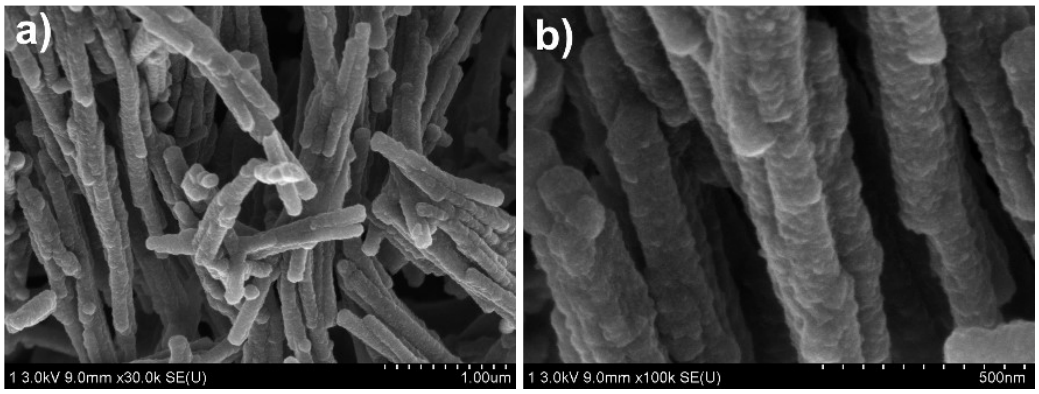

Fig. S1. FE-SEM images of FeNi-NCNT

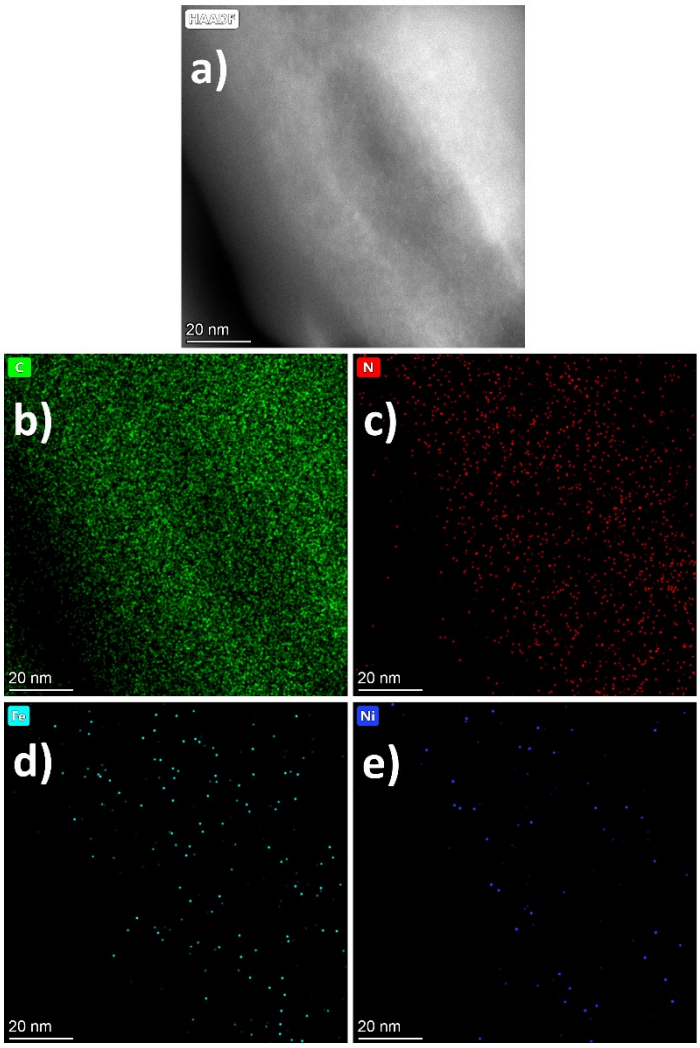

Fig. S2. a) STEM image of FeNi-NCNT, EDS elemental mapping of b) carbon, c) nitrogen, d) iron, e) nickel.

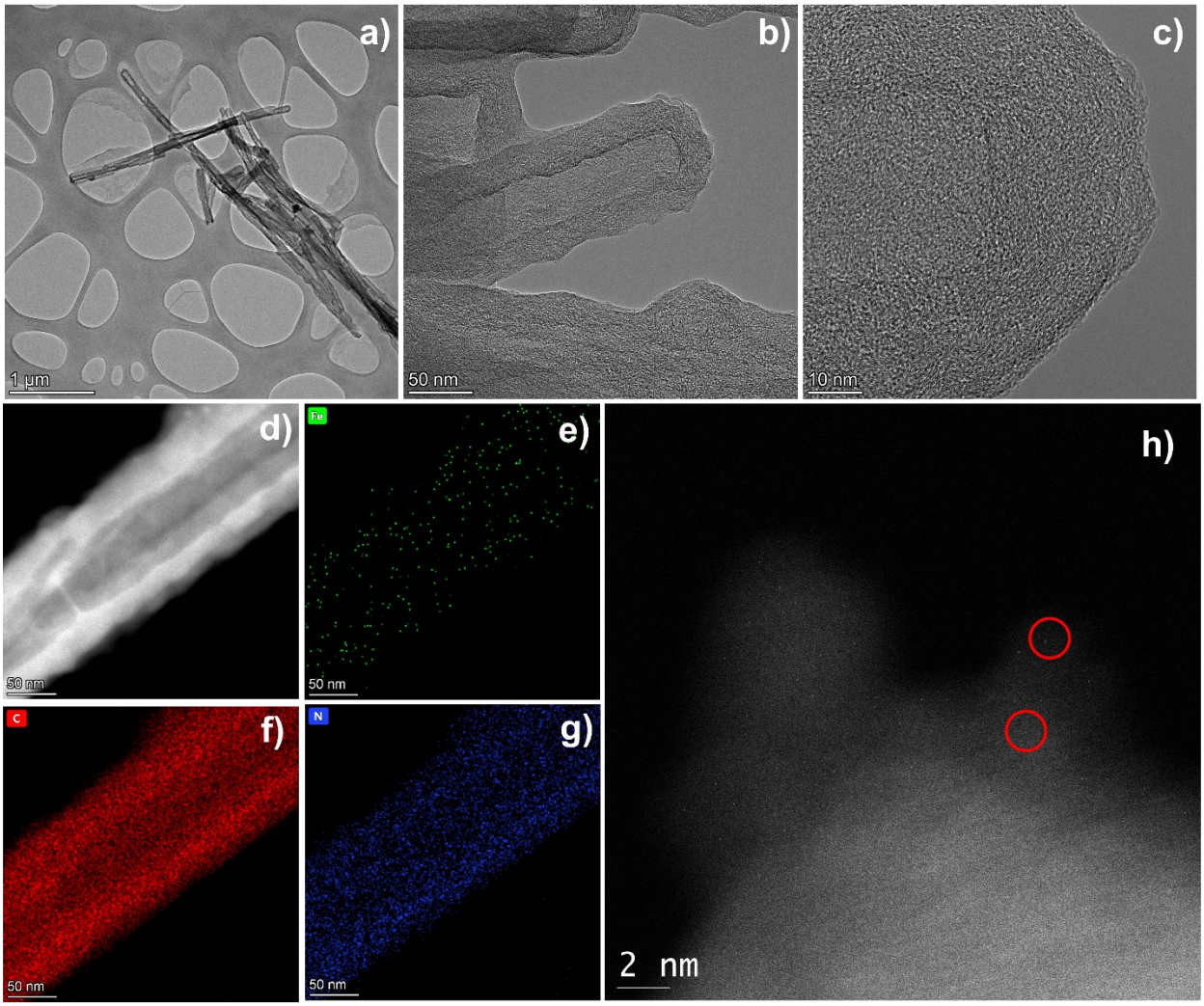

Fig. S3. a) TEM and b-c) high-resolution TEM images; d-g) STEM and EDS elemental mapping (Fe, C and N); h) HAADF-STEM image of the Fe-NCNT catalyst.

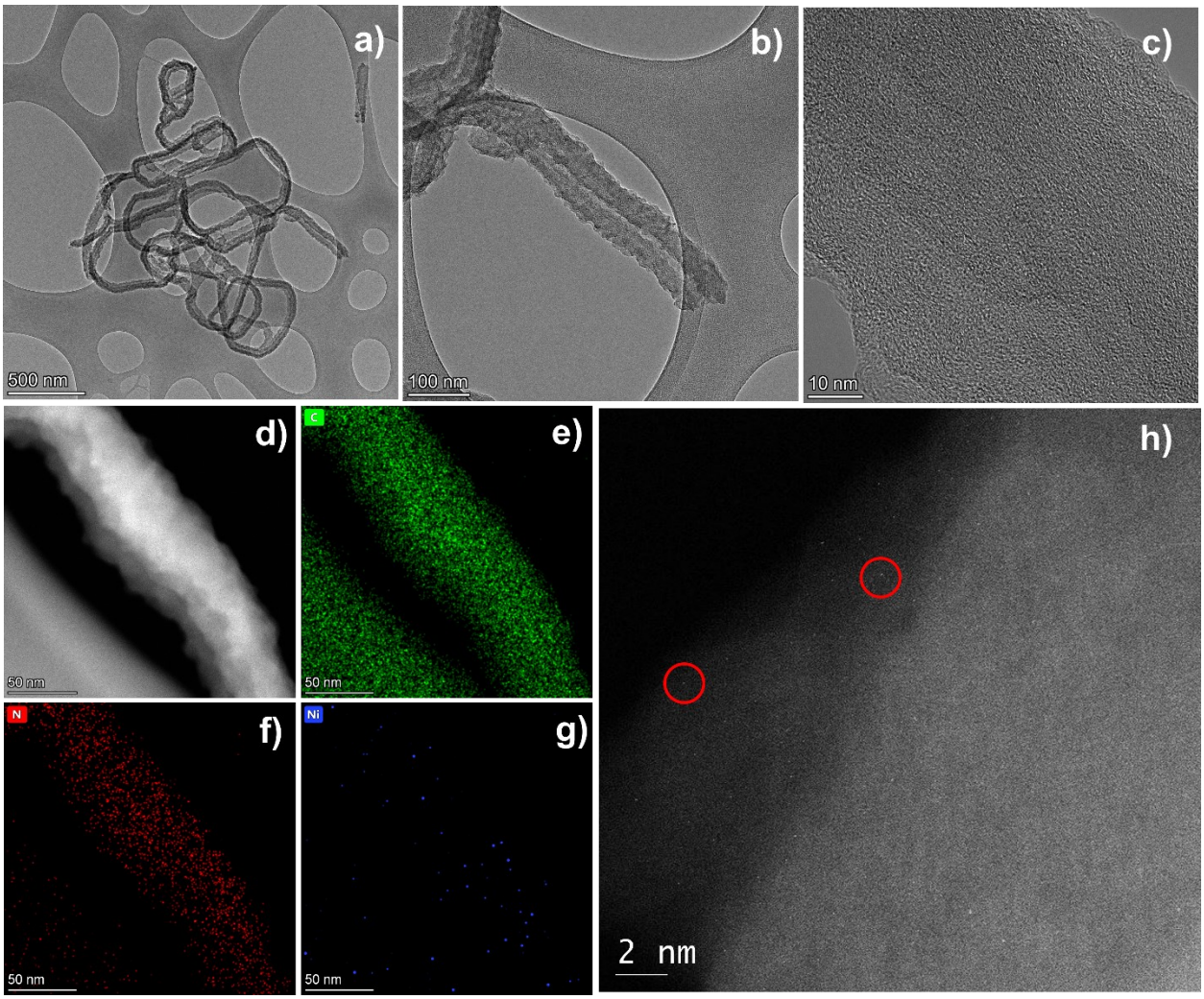

Fig. S4. a) TEM and b-c) high-resolution TEM images; d-g) STEM and EDS elemental mapping (C, N, and Ni); h) HAADF-STEM image of the Ni-NCNT catalyst.

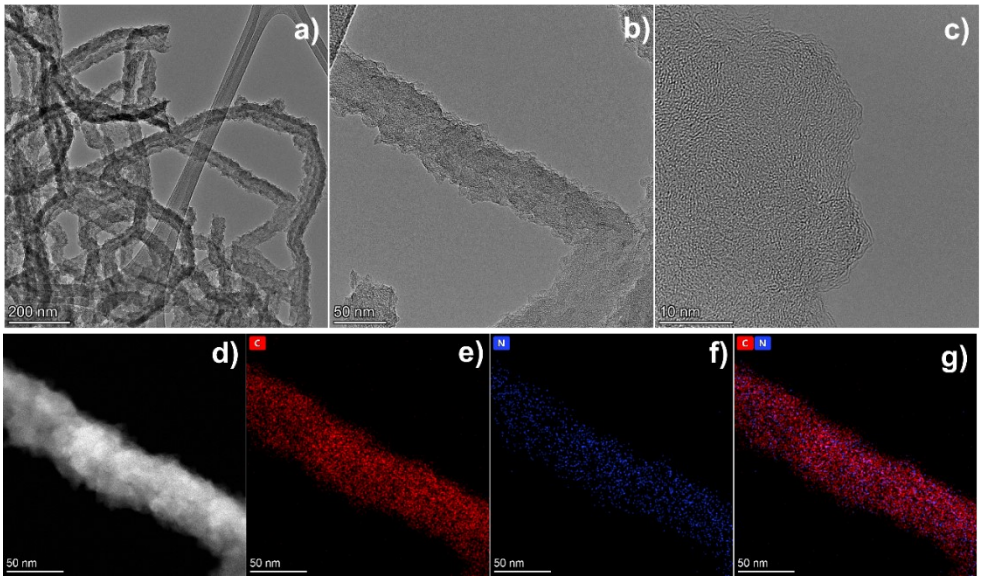

Fig. S5. a) TEM and b-c) high-resolution TEM images of NCNT; d-g) STEM and EDS elemental mapping of NCNT.

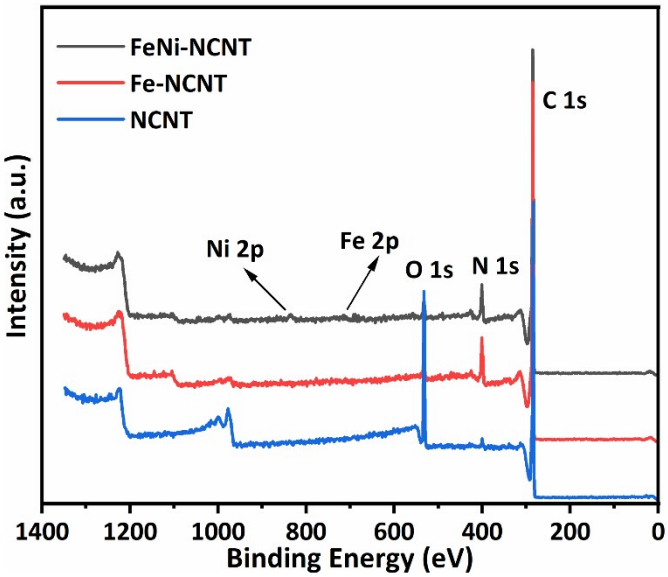

Fig. S6. XPS full-survey spectrum of all catalysts.

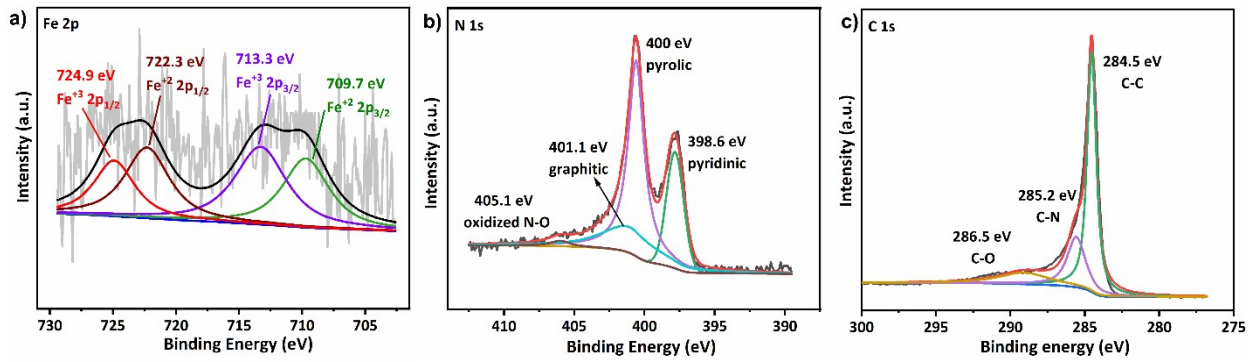

Fig. S7. High-resolution XPS spectra of a) Fe 2p, b) N 1s, and c) C 1s of the Fe-NCNT catalyst.

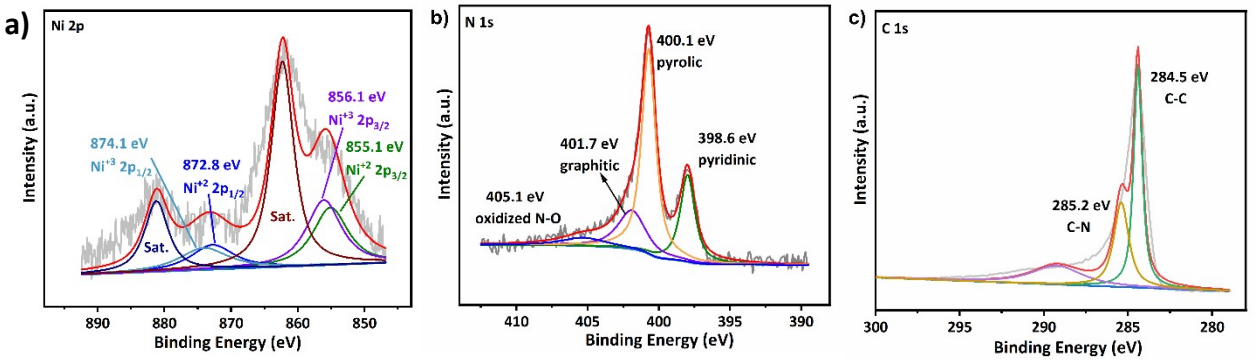

Fig. S8. High-resolution XPS spectra of a) Ni 2p, b) N 1s, and c) C 1s of the Ni-NCNT catalyst.

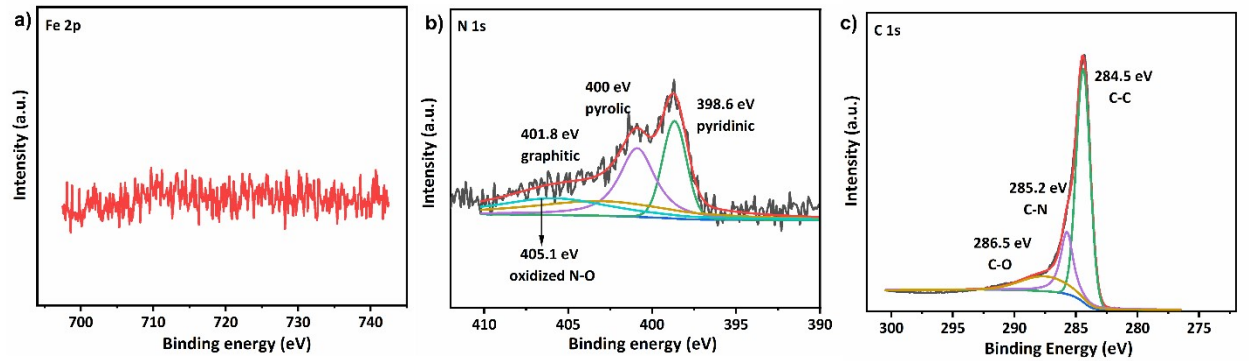

Fig. S9. High-resolution XPS spectra of a) Fe 2p, b) N 1s, and c) C 1s of the NCNT catalyst.

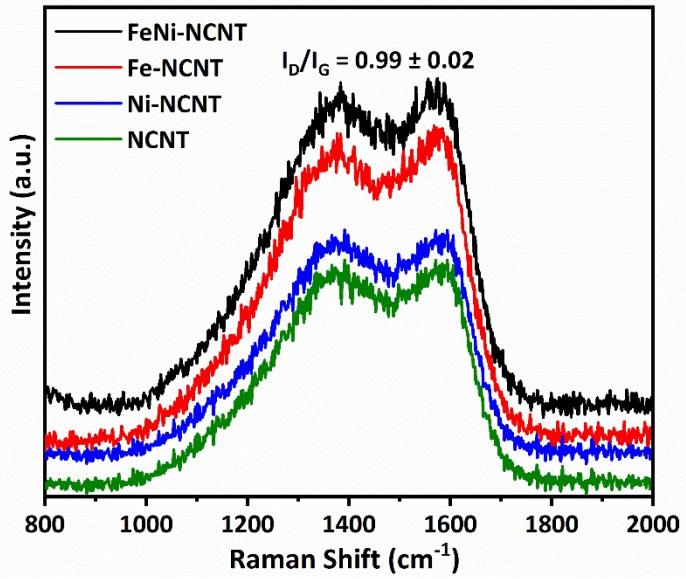

Fig. S10. Raman spectra of all the catalysts

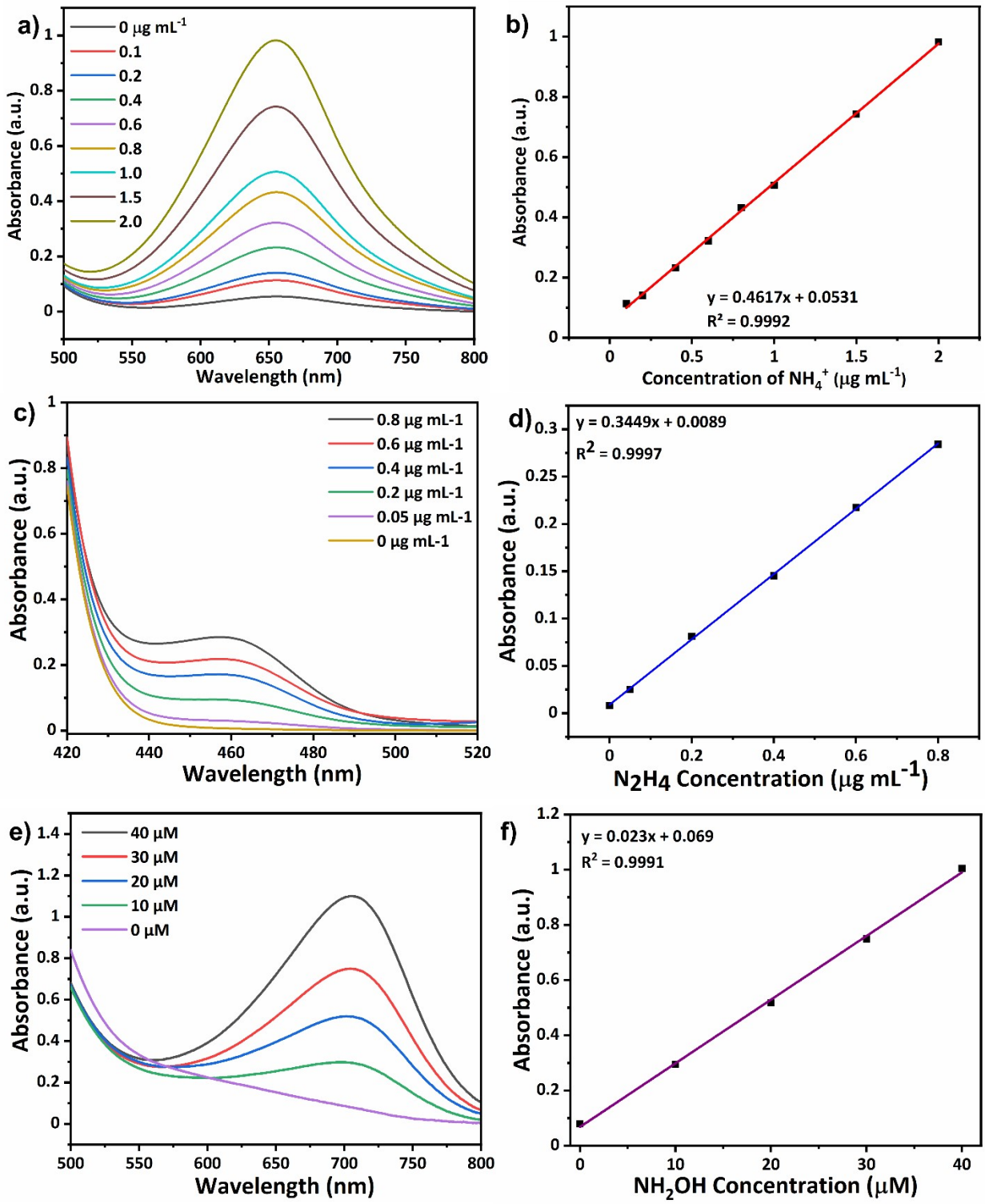

Fig. S11. UV-vis calibrations of NH_3, N_2H_4, and NH_2OH. a, b) UV-vis spectra and calibration curve of standard NH_3 solution, c, d) UV-vis spectra and calibration curve of standard N_2H_4 solution, e, f) UV-vis spectra and a calibration curve of standard NH_2OH solution.

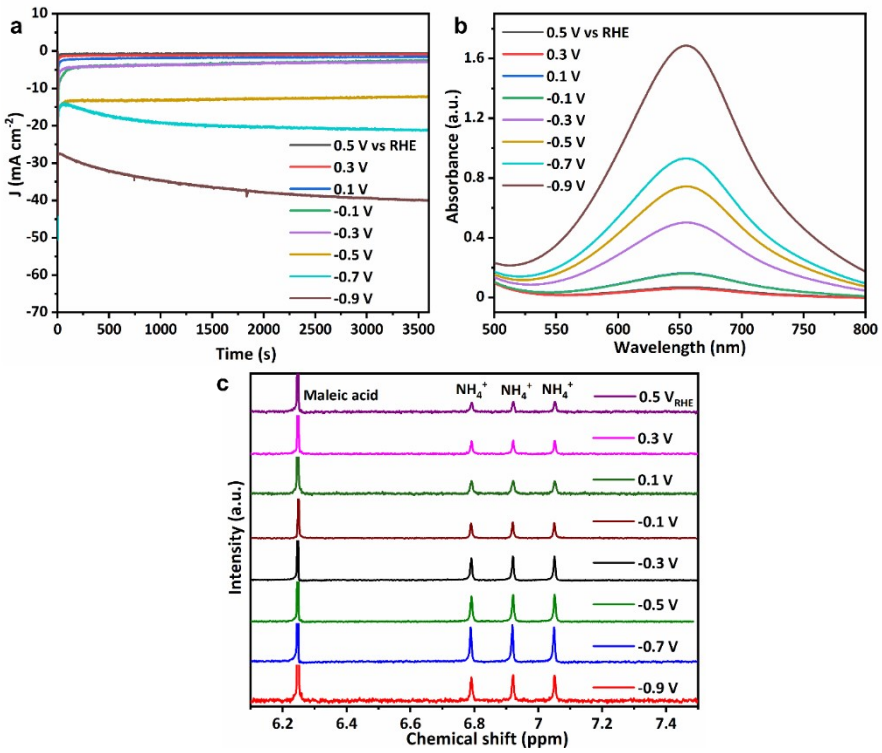

Fig. S12. The electrocatalytic performance of the FeNi-NCNT catalyst in NO-saturated 0.1 M HCl a) CA curves at various applied potentials. b) Corresponding UV-Vis absorbance and c) ^{1}H NMR chemical shift for NH_3 quantification. (The catholyte aliquots were diluted 10 times)

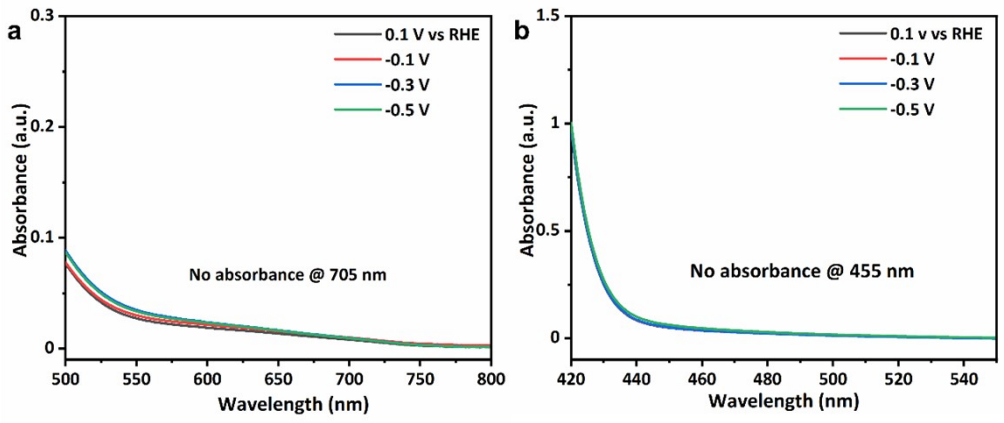

Fig. S13. UV-Vis absorbance curves of the FeNi-NCNT catalyst for a) NH_2OH, and b) N_2H_4 quantification

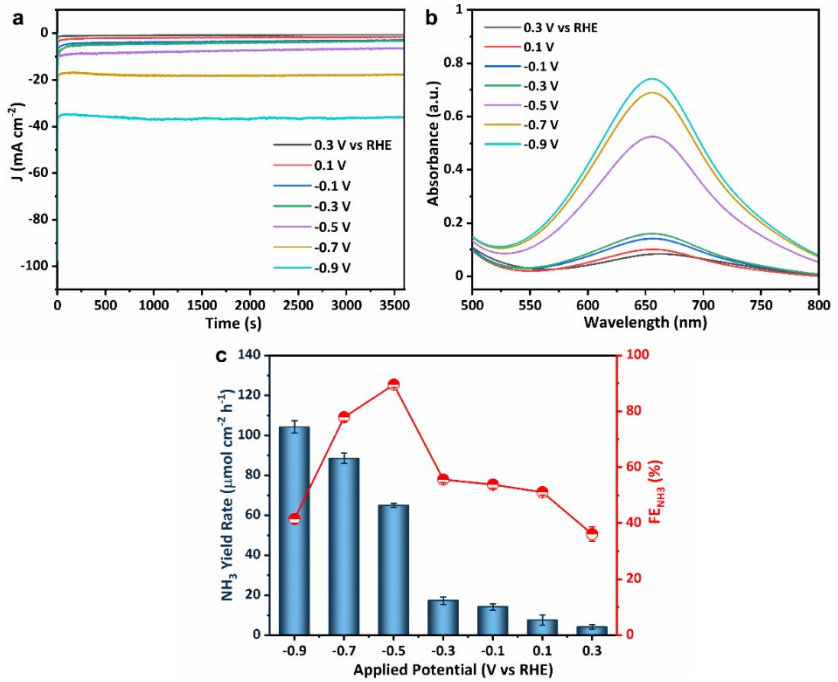

Fig. S14. The electrocatalytic performance of the Fe-NCNT catalyst in NO-saturated 0.1 M HCl a) CA curves at various applied potentials, b) UV-Vis absorbance for NH_3 quantification, and c) Corresponding NH_3 yield rate and FE_{NH3}. (The catholyte aliquots were diluted 10 times)

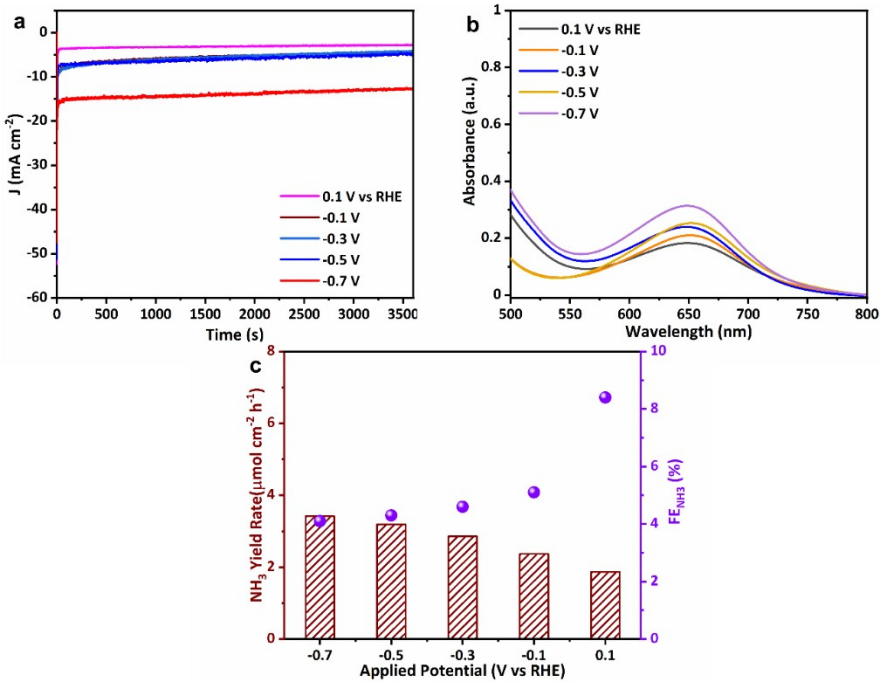

Fig. S15. The electrocatalytic performance of the NCNT catalyst in NO-saturated 0.1 M HCl a) CA curves at various applied potentials, b) UV-Vis absorbance for NH_3 quantification, and c) Corresponding NH_3 yield rate and FE_{NH3}.

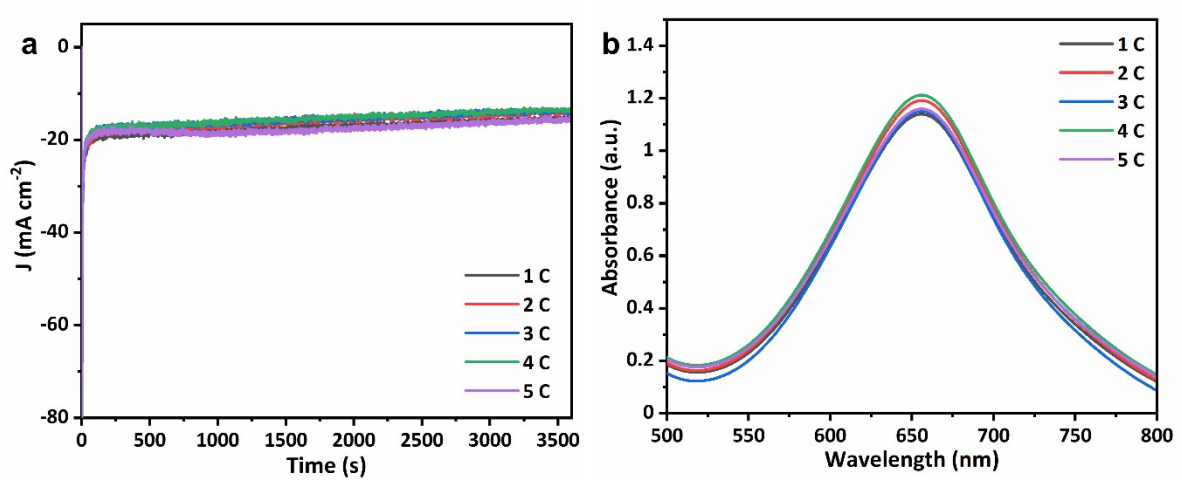

Fig. S16. Recycling stability study of the FeNi-NCNT catalyst in NO-saturated 0.1 M HCl a) CA curves obtained at -0.5 V_{RHE} and b) Corresponding UV-Vis absorbance for NH_3 quantification. (The catholyte aliquots were diluted 10 times)

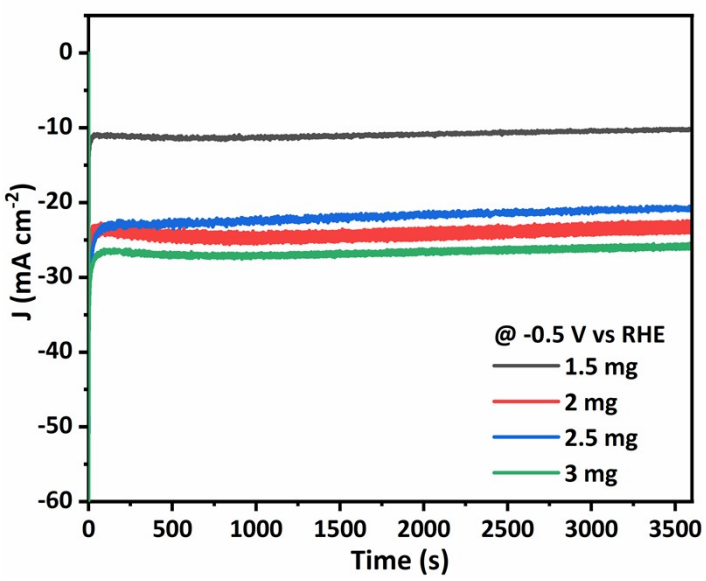

Fig. S17. CA curves obtained with varied catalyst loading at -0.5 V_{RHE}.

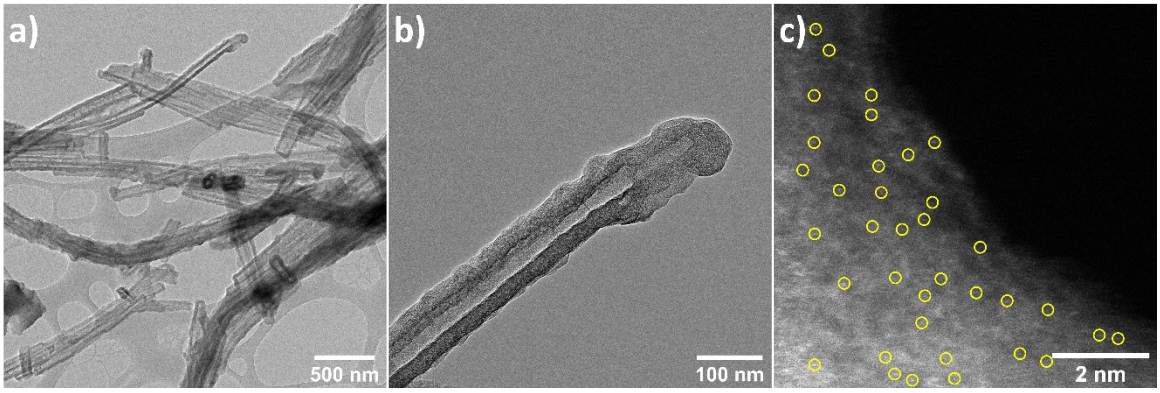

Fig. S18. Post HR-TEM analysis of FeNi-NCNT after the 50-h long-term durability test. (a, b) TEM images, (c) HAADF-STEM image

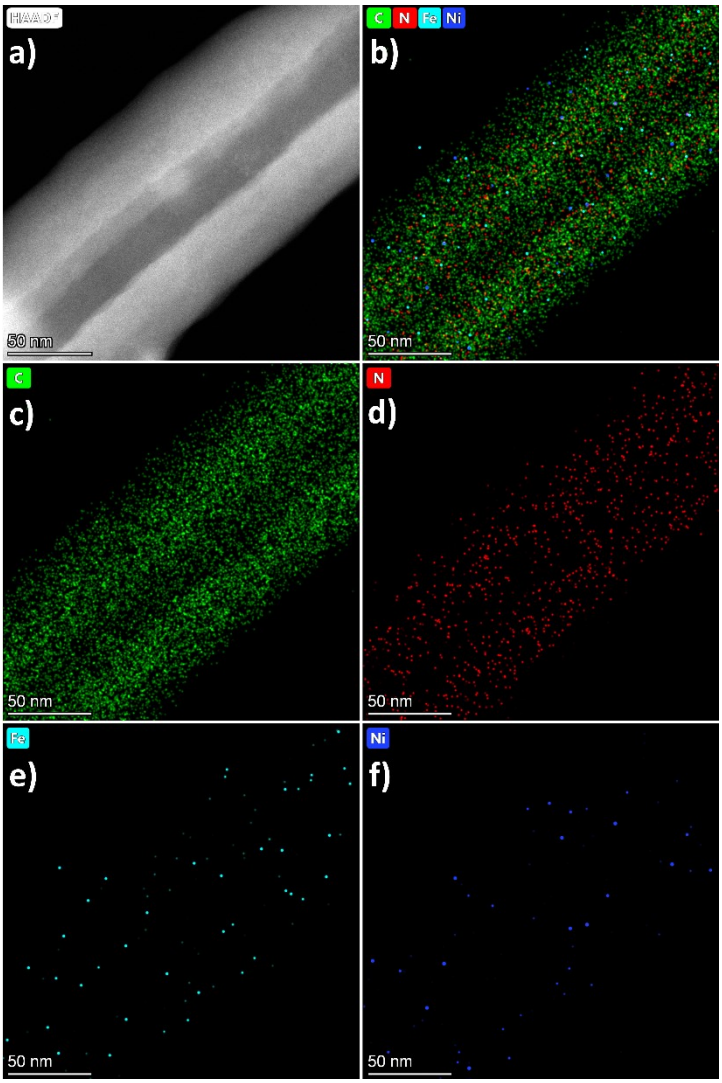

Fig. S19. Post EDS analysis of FeNi-NCNT after the 50-h long-term durability test. (a) STEM image of FeNi-NCNT, EDS elemental mapping of (b) carbon, (c) nitrogen, (d) iron, (e) nickel

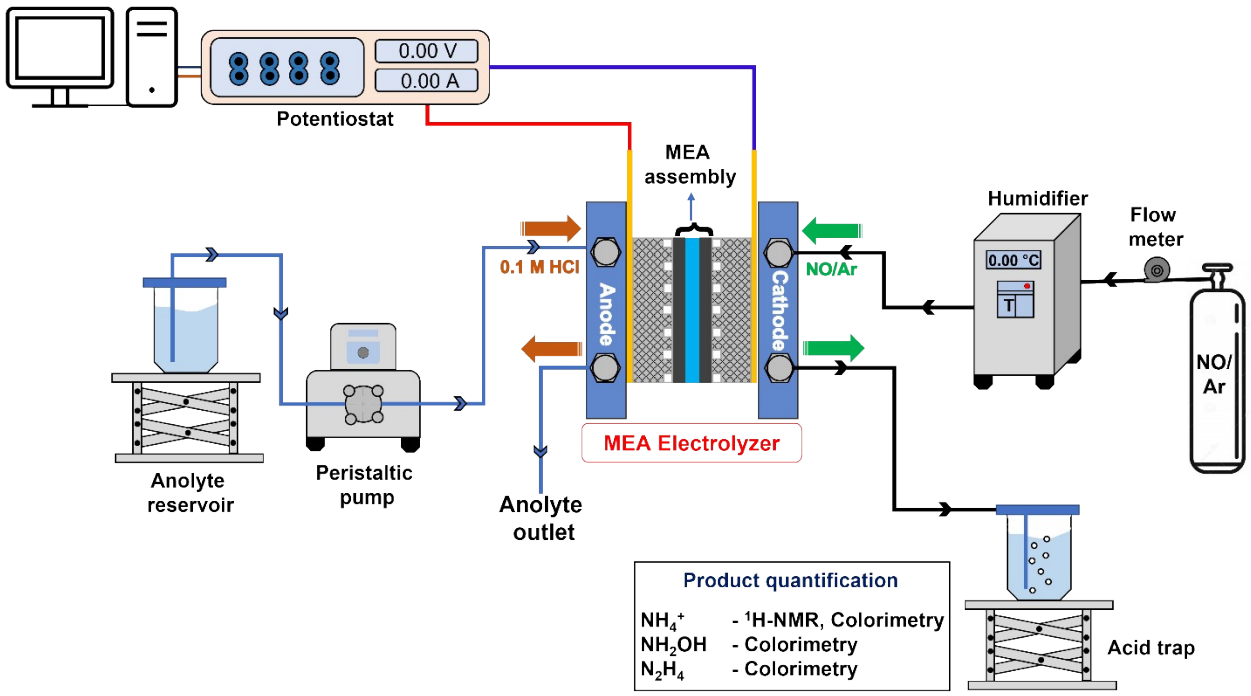

Fig. S20. Schematic of the MEA electrolyzer setup for NH_3 production in a NORR-OER full cell device.

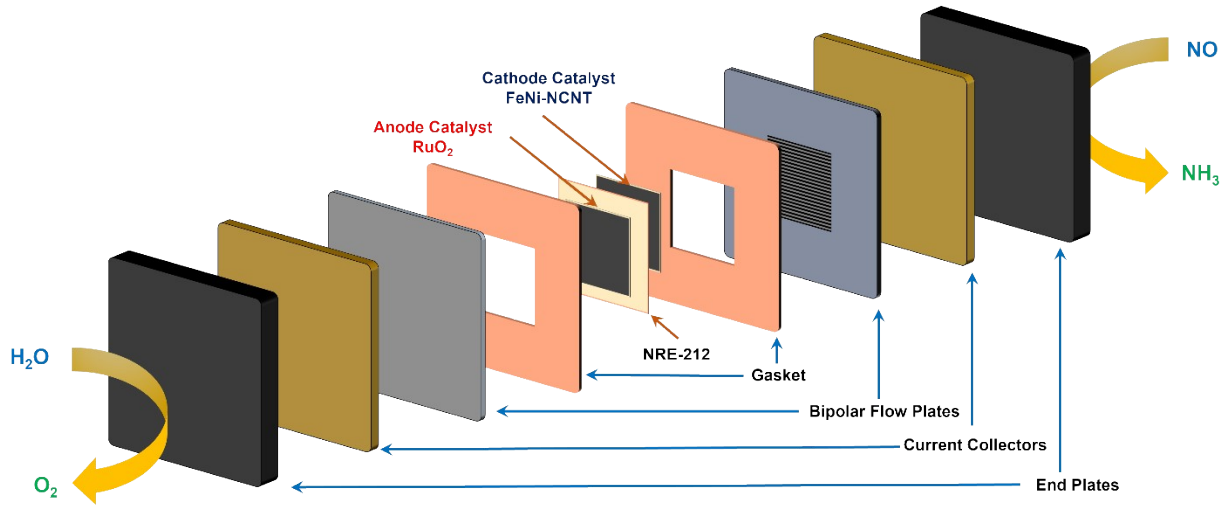

Fig. S21. Main components of the membrane electrode assembly electrolyzer utilized for the NORR-OER full cell operation.

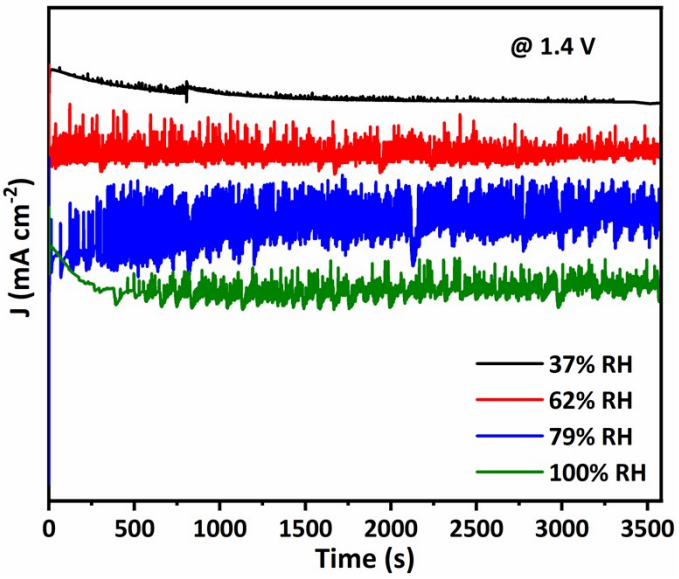

Fig. S22. Control experiment on the effect of water concentration on the eNORR performance of the FeNi-NCNT//RuO_2 MEA setup. a) CA curves obtained with various RH conditions at 1.4 V.

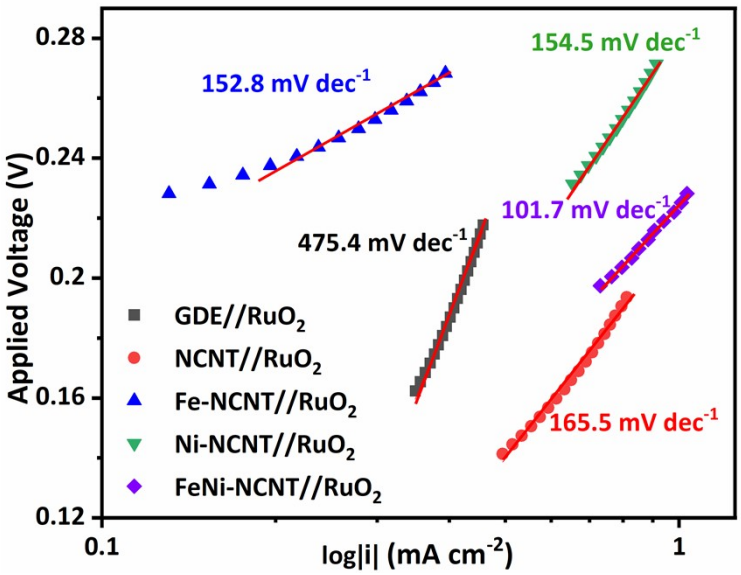

Fig. S23. Evaluation of a) Tafel Slope, and b) EIS of the various MEA system.

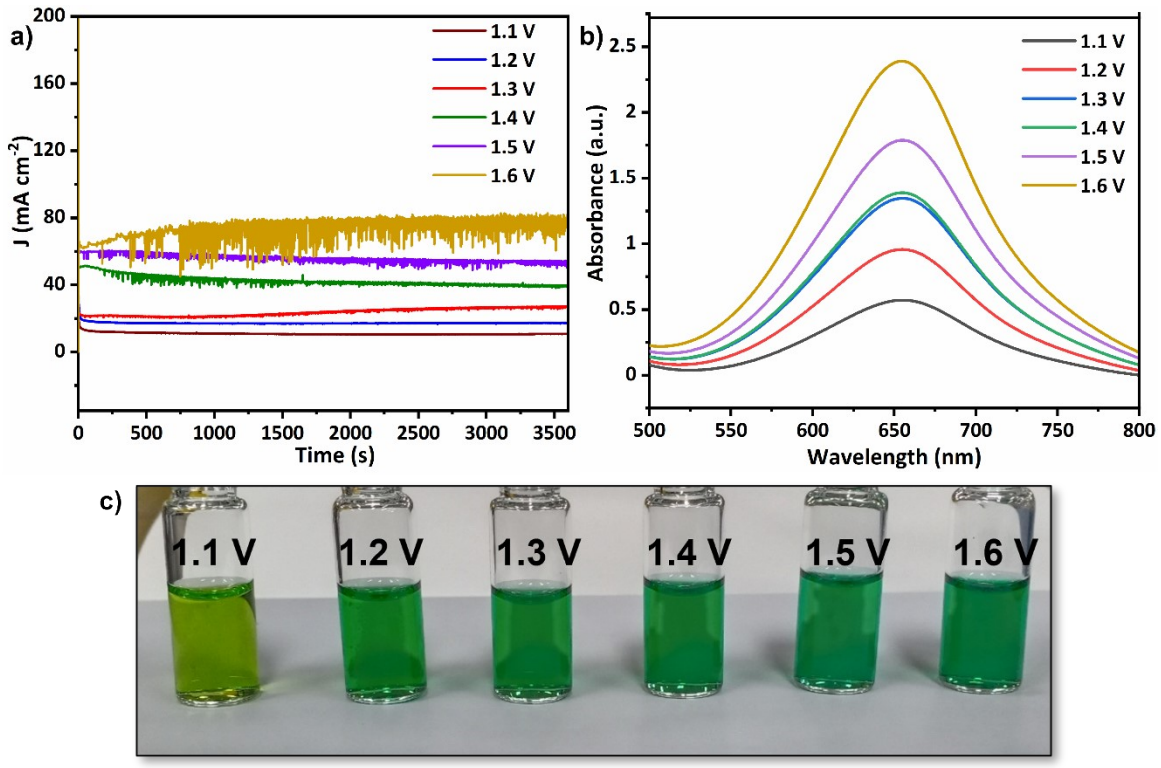

Fig. S24. Electrochemical evaluation of FeNi-NCNT//RuO_2 couple in MEA setup a) CA curves, b) Corresponding UV-Vis absorbance and c) Digital photographs of aliquots used for colorimetric quantification obtained at various applied voltages. (The catholyte aliquots were diluted 20 times)

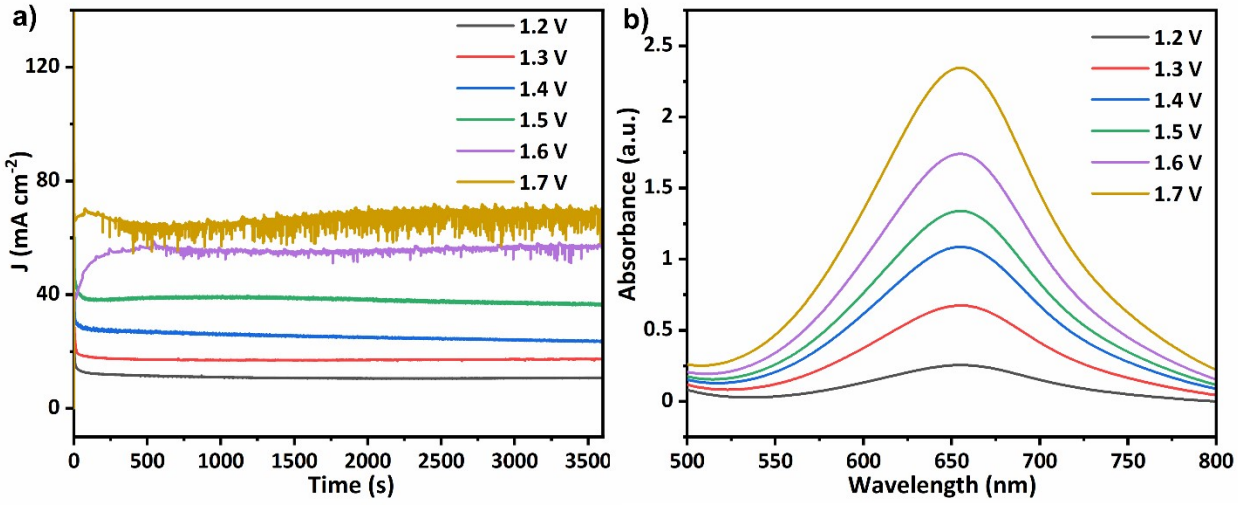

Fig. S25. Electrochemical evaluation of Fe-NCNT//RuO_2 couple in MEA setup a) CA curves, and b) Corresponding UV-Vis absorbance for NH_3 quantification at various applied voltages. (The catholyte aliquots were diluted 20 times)

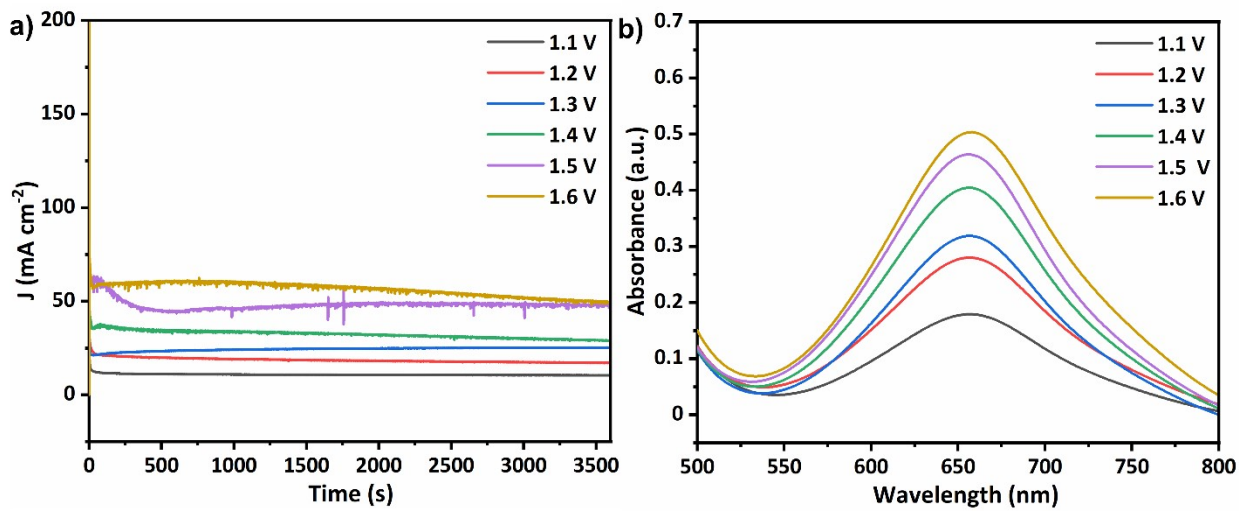

Fig. S26. Electrochemical evaluation of Ni-NCNT//RuO_2 couple in MEA setup a) CA curves, and b) Corresponding UV-Vis absorbance for NH_3 quantification at various applied voltages. (The catholyte aliquots were diluted 20 times)

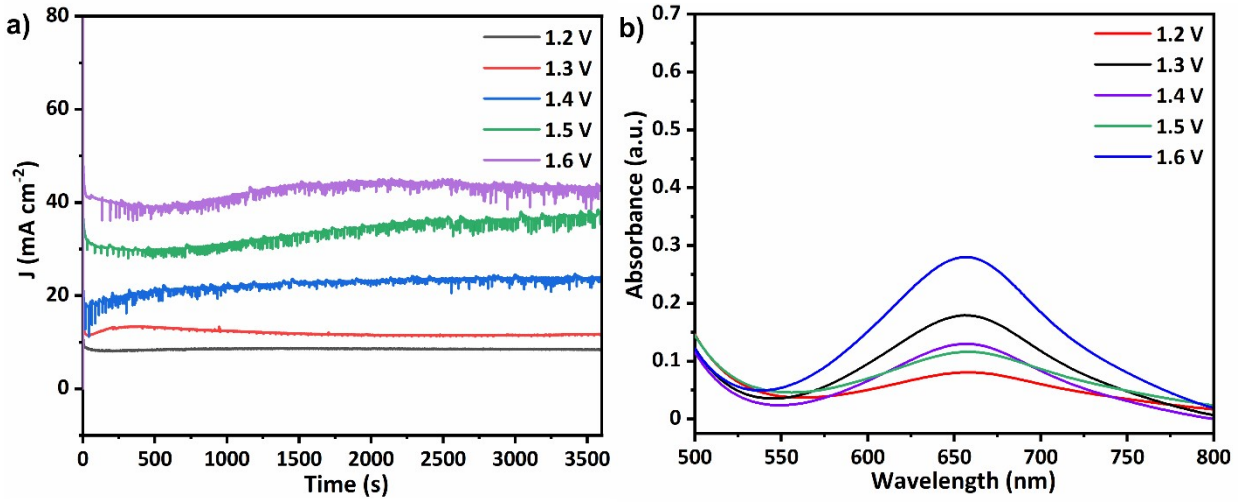

Fig. S27. Electrochemical evaluation of NCNT//RuO_2 couple in MEA setup a) CA curves, and b) Corresponding UV-Vis absorbance for NH_3 quantification at various applied voltages.

Table S1. Quantification of metal content in the catalysts using the ICP-OES technique.

Catalyst	Fe [wt%]	Ni [wt%]
FeNi-NCNT	0.53	0.34
Fe-NCNT	0.56	-
Ni-NCNT	-	0.31

Table S2. Comparison of eNORR performance of FeNi-NCNT in half-cell (H-type) batch electrolyzer conditions with reported aqueous-based eNORR catalysts.

Catalysts	**Potential** [Vs RHE]	**Electrolyte**	**NH_3 yield rate**	**FE_{NH3}** [%]	**Ref.**
FeNi-NCNT	**-0.5/-0.1**	**0.1 M HCl**	**76.2 μmol cm^{-2} h^{-1}/ 25.1 μmol cm^{-2} h^{-1}**	**92.6/ 88.7**	**This work**
Ni@NC	0.16	0.1 M HCl	34.6 μmol cm^{-2} h^{-1}	72.3	6
CoP/TM	-0.2	0.1 M Na_2SO_4	47.22 μmol cm^{-2} h^{-1}	88.3	7
NiNC@CF	-0.5	0.5 M PBS	94 μmol cm^{-2} h^{-1}	87	8
Ni_2P/CP	-0.2	0.1 M HCl	33.5 μmol cm^{-2} h^{-1}	76.9	9
Cu foil	-0.9	0.25 M Li_2SO_4	95.0 μmol cm^{-2} h^{-1}	61.9	10
MoS_2/GF	−0.7	0.1 M HCl + 0.5 mM Fe(II)SB	99.6 μmol cm^{-2} h^{-1}	~25	11
FeNC	-0.2	0.1 M $HClO_4$	20.2 μmol cm^{-2} h^{-1}	~5.1	12
Fe_2O_3/CP	-0.4	0.1 M Na_2SO_4	78.02 μmol cm^{-2} h^{-1}	86.73	13
NiO/TM	-0.6	0.1 M Na_2SO_4 + 0.05 mM Fe^{2+}-EDTA	125.3 μmol cm^{-2} h^{-1}	90	14
NiFe-LDH	-0.7	0.25 M Li_2SO_4	112 μmol cm^{-2} h^{-1}	82	15
Cu_2O@$CoMnO_4$	-0.8	0.1 M Na_2SO_4	94 μmol cm^{-2} h^{-1}	75.05	16
Ru-LCN	-0.2	0.5 M Na_2SO_4	45.02 μmol cm^{-2} h^{-1}	65.96	17
Co_1/MoS_2	-0.5	0.5 M Na_2SO_4	217.6 μmol cm^{-2} h^{-1}	87.7	18
Fe_1/MoS_{2-x}	-0.6	0.5 M Na_2SO_4	288.2 μmol cm^{-2} h^{-1}	82.5	19

Table S3. EIS analysis of the various MEA system.

MEA system	**R_{Ω} [Ω cm^2]**	**R_{ct} [Ω cm^2]**
FeNi-NCNT//RuO_2	0.02	0.15
Fe-NCNT//RuO_2	0.031	0.17
Ni-NCNT//RuO_2	0.033	0.24
NCNT//RuO_2	0.037	0.26
GDE//RuO_2	0.050	0.30

References

1. X. Yang, Z. Zhu, T. Dai and Y. Lu, *Macromol. Rapid. Commun.*, 2005, **26**, 1736–1740.

2. M. Tsipoaka, Md.A. Aziz and S. Shanmugam, *ACS Sustain Chem Eng.*, 2021, **9**, 2693–2704.

3. P.L. Searle, *Analyst*, 1984, **109**, 549–568.

4. G.W. Watt and J.D. Chrisp, *Anal. Chem.*, 1952, **24**, 2006–2008.

5. D.S. Frear and R.C. Burrell, *Anal. Chem.*, 1955, **27**, 1664–1665.

6. S. S. Markandaraj, T. Muthusamy and S. Shanmugam, *Adv. Sci.*, 2022, **9**, 2201410.

7. J. Liang, W.-F. Hu, B. Song, T. Mou, L. Zhang, Y. Luo, Q. Liu, A.A. Alshehri, M.S. Hamdy, L.-M. Yang and X. Sun, *Inorg. Chem. Front.*, 2022, **9**, 1366–1372.

8. T. Muthusamy, S. S. Markandaraj and S. Shanmugam, *J. Mater. Chem. A*, 2022, **10**, 6470–6474.

9. T. Mou, J. Liang, Z. Ma, L. Zhang, Y. Lin, T. Li, Q. Liu, Y. Luo, Y. Liu, S. Gao, H. Zhao, A.M. Asiri, D. Ma and X. Sun, *J. Mater. Chem. A*, 2021, **9**, 24268–24275.

10. J. Long, S. Chen, Y. Zhang, C. Guo, X. Fu, D. Deng and J. Xiao, *Angew. Chem., Int. Ed.*, 2020, **59**, 9711–9718.

11. L. Zhang, J. Liang, Y. Wang, T. Mou, Y. Lin, L. Yue, T. Li, Q. Liu, Y. Luo, N. Li, B. Tang, Y. Liu, S. Gao, A.A. Alshehri, X. Guo, D. Ma and X. Sun, *Angew. Chem., Int. Ed.*, 2021, **60**, 25263–25268.

12. D.H. Kim, S. Ringe, H. Kim, S. Kim, B. Kim, G. Bae, H.-S. Oh, F. Jaouen, W. Kim, H. Kim and C.H. Choi, *Nat. Commun.,* 2021, **12**, 1856.

13. J. Liang, H. Chen, T. Mou, L. Zhang, Y. Lin, L. Yue, Y. Luo, Q. Liu, N. Li, A.A. Alshehri, I. Shakir, P.O. Agboola, Y. Wang, B. Tang, D. Ma and X. Sun, *J. Mater. Chem. A*, 2022, **10**, 6454–6462.

14. P. Liu, J. Liang, J. Wang, L. Zhang, J. Li, L. Yue, Y. Ren, T. Li, Y. Luo, N. Li, B. Tang, Q. Liu, A.M. Asiri, Q. Kong and X. Sun, *Chem. Commun.*, 2021, **57**, 13562–13565.

15. G. Meng, T. Wei, W. Liu, W. Li, S. Zhang, W. Liu, Q. Liu, H. Bao, J. Luo and X. Liu, *Chem. Commun.*, 2022, **58**, 8097–8100.

16. C. Bai, S. Fan, X. Li, Z. Niu, J. Wang, Z. Liu and D. Zhang, *Adv. Funct. Mater.*, 2022, **32**, 2205569.

17. Y. Li, C. Cheng, S. Han, Y. Huang, X. Du, B. Zhang and Y. Yu, *ACS Energy Lett.*, 2022, **7**, 1187–1194.

18. X. Li, K. Chen, X. Lu, D. Ma and K. Chu, *Chem. Eng. J.*, 2023, **454**, 140333.

19. K. Chen, J. Wang, J. Kang, X. Lu, X. Zhao and K. Chu, *Appl. Catal. B*, 2023, **324**, 122241.